Band structure and heat capacity of low-coverage helium films on noble-gas-plated graphite

Carey Schwartz
Physics Division, Michelson Laboratory (Code 3813), U.S. Naval Weapons Center, China Lake, California 93555

Milton W. Cole
Department of Physics, The Pennsylvania State University, University Park, Pennsylvania 16802

(Received 9 January 1986)

Calculations are presented of the energy band structure of ^{4}He atoms moving across the surface of a monolayer of Ar, Kr, or Xe adsorbed on graphite. The results are very sensitive to adsorbate density, allowing the possibility of experimentally varying the degree of He localization. From the dispersion relation, the density of states and low-coverage heat capacity are computed. In the case of Ar plating, agreement is obtained with the isosteric heat measurement of Lerner and Daunt. Speculation is made that the heat-capacity data of Crary *et al.* are influenced by Ar atoms on the second layer. In the case of Kr plating, satisfactory agreement is obtained with the data of Tejwani, Ferreira, and Vilches.

I. INTRODUCTION

The behavior of physically adsorbed, submonolayer films varies considerably with the adsorbing surface. In some cases, the only role of the substrate is to confine the atoms to a plane. Such systems exhibit properties of ideal, two-dimensional (2D) matter. In other cases, the periodicity of the adsorbate imposes, for example, diverse commensurate and incommensurate structures at low temperature.[1–4] Predicting this variability is a challenge for the theory.[5,6]

One of the most interesting kinds of adsorption system is produced by depositing noble gases on graphite, and then superposing a variable coverage of helium. This results in a controllable variation of the 2D helium properties. This is demonstrated in Fig. 1 in which substantial differences are found in the specific heat of helium at low temperature T. For example, the peaks seen in the specific heat of helium adsorbed on either argon or krypton plated graphite are interpreted as demonstrating the coexistence of 2D vapor and commensurate phases.[1,4,5] At moderately high T, $\sim$4 K, the heat capacity approaches the 2D ideal-gas limit $C_{2D}/Nk_B = 1$. Finally, at higher T than is shown in Fig. 1, excitation of surface-normal motion causes C to rise above C_{2D}.[7–9]

The theoretical interpretation of such data requires, in general, the application of statistical mechanics to the problem of a strongly interacting quantum system in an external field. Rather than solve this intractable problem, some theoretical efforts have utilized perturbation expansions in the substrate field and/or the helium-helium interaction.[5–8] The work reported here employs an alternative route of neglecting completely the helium-helium interaction but evaluating "exactly" the role of the substrate. Further work may be directed toward systematic improvement along the lines followed by Rehr, Bruch, and their co-workers.[5,6,8]

Our approach consists of a numerical evaluation of the band structure of a helium atom in the potential presented by a rare gas adlayer on graphite. This yields a specific heat which can, in principle, be compared to the low helium coverage extrapolation of the data. This route has been followed for helium adsorbed on bare graphite.[7–9]

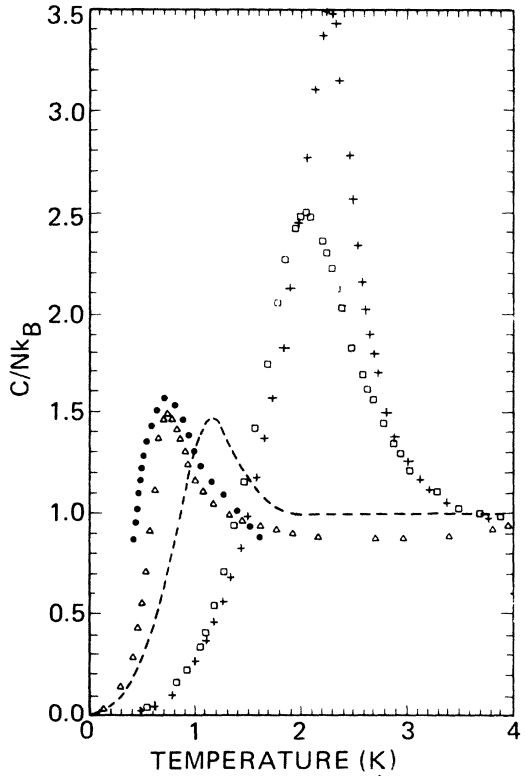

FIG. 1. Heat capacity per atom of a ^{4}He film at coverage near 0.025 Å^{-2} on bare graphite (dashed line) and graphite plated with a monolayer of ^{4}He (●), Ne (△), Ar (+), and Kr (□). Figure taken from Crary *et al.*, Ref. 4, using data from Refs. 3 and 4.

Calculations similar to these were performed some years ago by Novaco and Milford for the cases of argon and xenon adlayers.[10,11] Our calculations for these adsorbates differ in the numerical techniques employed, in the overlayer density, and in the use of different atom-surface potentials, revised in accordance with current understanding of gas-gas[12] and gas-surface[13–15] interactions. The interaction potentials used in this work have been found to be consistent[14–16] with diffractive helium scattering experiment results.[17]

II. CALCULATIONS

We have used the method of Ref. 7., which expands the wave function $\psi_{\mathbf{K}}$ of the helium atom in a complete set of states

$$\psi_{\mathbf{K}}(\mathbf{R},z)=\sum_{n,\mathbf{G}}\alpha_{n\mathbf{G}}\phi_n(z)e^{i(\mathbf{K}+\mathbf{G})\cdot\mathbf{R}}, \tag{1}$$

where the position of the helium atom is $\mathbf{r}=(\mathbf{R},z)$, the z axis is perpendicular to the surface and $\mathbf{R}$ is a vector which lies in the plane of the surface. The wave vector $\mathbf{K}$ also lies in the plane of the surface and $\mathbf{G}$ is a 2D reciprocal lattice vector chosen from the set

$$\mathbf{G}_{mn}=n\mathbf{G}_1+m\mathbf{G}_2 . \tag{2}$$

The basis vectors $\mathbf{G}_1$ and $\mathbf{G}_2$ differ in direction by 60° and have magnitude $G_1=4\pi/(\sqrt{3}a)$; a is the separation of the adsorbed rare-gas atoms. In the commensurate configuration assumed here for krypton and xenon, $a=4.26$ Å and hence $G_1=1.70$ Å^{-1}. For argon monolayers a is taken to be 3.97 Å which reflects the smaller size of argon relative to either krypton or xenon.[18] In Eq. (1) the basis functions ϕ_n are chosen to be the eigenfunctions of the one-dimensional Schrödinger equation for a helium atom in the potential $V_0(z)$

$$\left[-\frac{\hbar^2}{2m}\frac{d^2}{dz^2}+V_0(z)\right]\phi_n(z)=\varepsilon_n\phi_n(z) . \tag{3}$$

Here $V_0(\mathbf{z})$ is the leading term in the Fourier expansion of the helium-substrate potential,

$$V(\mathbf{r})=V_0(z)+\sum_{\mathbf{G}(\neq 0)}V_{\mathbf{G}}(z)\exp(i\mathbf{G}\cdot\mathbf{R}) . \tag{4}$$

Combining Eqs. (1), (3), and (4) yields

$$\sum_{n',G'}\left[\left[\varepsilon_n+\frac{\hbar^2}{2m}(\mathbf{K}+\mathbf{G})^2\right]\delta_{\mathbf{G},\mathbf{G}'}\delta_{nn'}+\langle n\mid V_{\mathbf{G}-\mathbf{G}'}\mid n'\rangle\right]\alpha_{n'\mathbf{G}'}=\alpha_{n\mathbf{G}}E , \tag{5a}$$

$$\langle n\mid V_{\mathbf{G}-\mathbf{G}'}\mid n'\rangle=\int dz\,\phi_n(z)V_{\mathbf{G}-\mathbf{G}'}(z)\phi_{n'}(z) . \tag{5b}$$

Equation (5a) is one of a set of infinitely many coupled equations for the $\mathbf{K}$ dependent amplitudes $\alpha_{n\mathbf{G}}$ and energy eigenvalues E. It is the latter with which we concern ourselves. Note that states involving different n and $\mathbf{G}$ are coupled via matrix elements of the corrugation. By standard matrix inversion techniques, these equations can be solved numerically for both the partial wave amplitudes and eigenvalues. The only difference between the method reported in Ref. 7 and the current procedure is that the former employed bound state energies and matrix elements determined from experiment,[19] whereas we calculate these quantities from Eqs. (3) and (4) directly. In fact, the demonstrated consistency of $V(\mathbf{r})$ with diffractive scattering data from rare-gas overlayers suggests that this is a reliable procedure.[14–17]

The key input to the problem is the atom-substrate potential $V(\mathbf{r})$. We use the potentials developed by Chung, *et al.*[15] Briefly, these are of the form

$$V(\mathbf{r})=V_a+V_s+V_3^{a-a}+V_3^{a-s}, \tag{6}$$

with V_a the interaction of a helium atom with a rigid adlayer, V_s the potential due to the underlying graphite substrate, V_3^{a-a} the result of three-body interactions between pairs of overlayer atoms and the adsorbed helium, and V_3^{a-s} due to substrate-adatom-He three-body interactions. The last three terms in Eq. (6) are assumed to contribute only to the lateral average of the potential, i.e., the term V_0 in Eq. (4). The term V_a contributes to both the lateral average and the corrugation in the potential. It is derived from a pairwise summation of the He-adsorbate interactions. Note for later use that we have calculated all the Fourier components of the potential for which $G_{mn}\leq 3G_1$.

With the potential fully specified, we then use standard numerical techniques to solve Eq. (3) for both the energy eigenvalues and the corresponding normalized wave functions.[20] It is then straightforward to calculate the various matrix elements which occur in Eq. (5). In order to solve Eq. (5) we truncate the number of equations by limiting the basis set to those reciprocal-lattice vectors for which $G_{mn}\leq 2G_1$, and to the four deepest bound states of Eq. (3). This leads to a basis of size 76. The resulting 76 coupled equations are then solved on a grid in the irreducible Brillouin zone, Fig. 2, for the energy eigenvalues.

The results for the band structures of helium on argon and krypton plated graphite are shown in Figs. 2 and 3. The band structure which results for helium on xenon plated graphite is nearly identical to that of krypton-plated graphite, as expected from their similar interactions with helium.[15] In obtaining these results we have used for the helium-adsorbate interactions a Maitland-Smith potential with two-body well depth of 29.4, 30.4, and 27.4 K for the adatoms Ar, Kr, and Xe.[12,21] The corresponding equilibrium distances are $r_m=3.43$, 3.64, and 3.98 Å, respectively. As seen in Table I, the binding energy ε_0 agrees within 2% for these cases. This is a result of the weaker attraction in the xenon-helium case being compensated for by its greater spatial extent than the other cases; of course this conclusion is a consequence also of the monolayer densities.

Some of the results reported in Table I and Figs. 2 and 3 can be interpreted qualitatively in terms of perturbation theory. Near the ground state, at the Γ point, this gives

$$E\simeq\varepsilon_0-\sum_{n\mathbf{G}}\frac{|\langle n\mid V_{\mathbf{G}}\mid 0\rangle|^2}{\varepsilon_n-\varepsilon_0+\hbar^2(G^2+2\mathbf{K}\cdot\mathbf{G})/2m} . \tag{7}$$

Near $\mathbf{K}=0$, this may be expanded to obtain

TABLE I. ^{4}He energy levels with and without band-structure effects; all energies are expressed in kelvin. ε_0 is the ground-state eigenvalue of $V_0(z)$; $E_0-\varepsilon_0$ is the band-structure shift computed here (or in Ref. 7 for the case of bare graphite). The calculated effective mass enhancement is m^*/m and $\langle 0 \mid V_1 \mid 0 \rangle$ is the expectation value of the lowest nonzero **G** Fourier component of the potential.

Substrate	ε_0 Theory	ε_0 Experiment	$E_0-\varepsilon_0$	E_0 Theory	E_0 Experiment	m^*/m	$\langle 0 \mid V_1 \mid 0 \rangle$
Bare graphite		144±0.6[a]	−1.4[b]		143±2[c]	1.06	3.2[a]
Ar/graphite	−56.7[d]		−5.3	−62.0 (−71[e])	−69±4[f]	1.20	−5.1[d]
Kr/graphite	−55.2[d]	−54±1.6[g]	−5.7	−60.9		1.23	−5.7[d]
Xe/graphite	−56.1[d]	−56±1.7[h]	−5.1	61.2		1.22	−5.2[d]

[a]From Ref. 19.
[b]From Ref. 20.
[c]From Ref. 9.
[d]From Ref. 15.
[e]Derived in the text at Ar density 0.087 Å^{-2} used in the experiment of Ref. 2.
[f]Derived from the isoteric heat data of Ref. 2 as described in the text.
[g]From Larese *et al.*, Ref. 17.
[h]From Bracco *et al.*, Ref. 17.

$$E \simeq E_0 + \hbar^2 K^2/2m^* \,. \tag{8}$$

The lowest-order approximation neglects the contribution of terms for which $n \neq 0$ and **G** values wih magnitude greater than G_1. The result then includes only six terms and is

$$E_0 \simeq \varepsilon_0 - 6 \mid \langle 0 \mid V_1 \mid 0 \rangle \mid \lambda \,, \tag{9a}$$

$$m^*/m \simeq 1 + 12\lambda^2 \,, \tag{9b}$$

$$\lambda \equiv 2m \mid \langle 0 \mid V_1 \mid 0 \rangle \mid /\hbar^2 G_1^2 \,, \tag{9c}$$

and V_1 corresponds to G_1. λ is an expansion parameter in the theory.

For a Kr adlayer, the energy shift at the center of the zone is thus predicted to be $E_0-\varepsilon_0=-9$ K, a factor of nearly 2 larger than the actual value presented in Table I. The effective mass m^*/m calculated with Eq. (9b) is ~ 2 while Table I reveals a value of 1.2. Another prediction of this perturbation theory is that the gap at the M point is $2 \mid \langle 0 \mid V_1 \mid 0 \rangle \mid = 10$ K, more than twice the result shown in Fig. 2. These inaccuracies of second-order perturbation theory were not observed in the bare graphite case,[7] for which the parameter λ assumes the value of

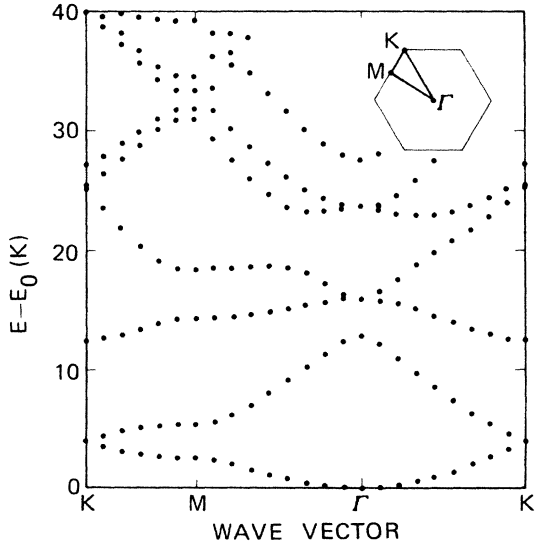

FIG. 2. Band structure of He on Kr-plated graphite along the lines ΓM, MK, and ΓK in Brillouin zone, shown at upper right. Energy is measured relative to the ground state value E_0 in Table I.

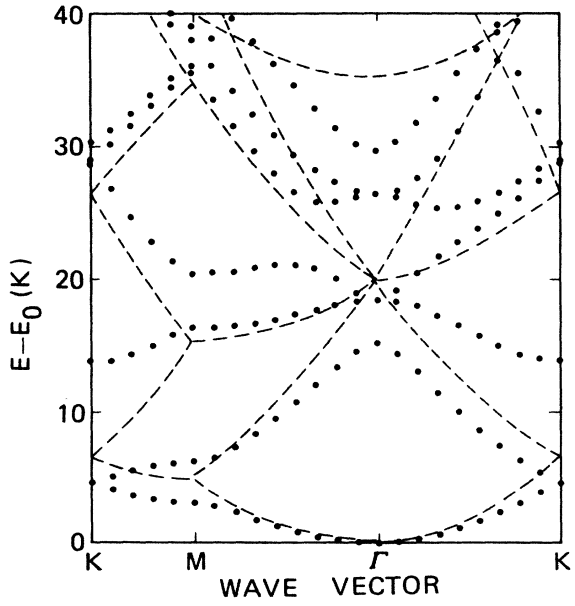

FIG. 3. Band structure of He on Ar-plated graphite. Notation same as Fig. 2. Dashed curve is spectrum obtained in the hypothetical case when the matrix elements of the periodic potential are set equal to zero in Eq. (5a); in that case the value of E_0 is ε_0.

0.06, instead of 0.3 in the present case. This difference arises from the much larger corrugation[14–17] and the factor of $\sqrt{3}$ smaller value of G_1 in the overlayer case.

We turn next to the density of states per unit area

$$g(E)=A^{-1}\sum_{\nu\mathbf{K}}\delta(E-E_{\nu\mathbf{K}})\ . \tag{10}$$

This may be computed from the solutions of Eq. (5) for sufficiently many **K** values. The fluctuations in the results, shown in Figs. 4 and 5, are due to the finite number ($\sim$8000) of **K** values which are evaluated. These figures show for reference a strictly 2D density of states g_0 and the form of a smooth surface approximation to Eq. (10), $g_{sm}(E)$:

$$g_0=m/(2\pi\hbar^2)\ , \tag{11a}$$

$$g_{sm}(E)=g_0\sum_n\Theta(E-\varepsilon_n)\ . \tag{11b}$$

In the latter expression one sees Heaviside-step-function contributions $\Theta(E-\varepsilon_n)$ corresponding to the threshold behavior for excitation of vibration perpendicular to the surface.

One observes in the results for $g(E)$ an effective mass enhancement at very low E [i.e., $g(E)/g_0>1$] and zone boundary splittings at higher E. Especially important at low T are the minima in $g(E)$ near $E-E_0\simeq 5$ and 13 K. Because of the larger corrugation these splittings are larger than in the graphite case[7] except at the **K** point. To understand this exception it suffices to consider the equations of the form (5) involving the three vectors **G**(0 and two others) which would give degenerate states (**K**+**G**) at the K point if there were no corrugation. In the presence of coupling, the solution of these equations yields energy shifts

$$E_K-\frac{\hbar^2K^2}{2m}\simeq 2V,-V,-V\ , \tag{12}$$

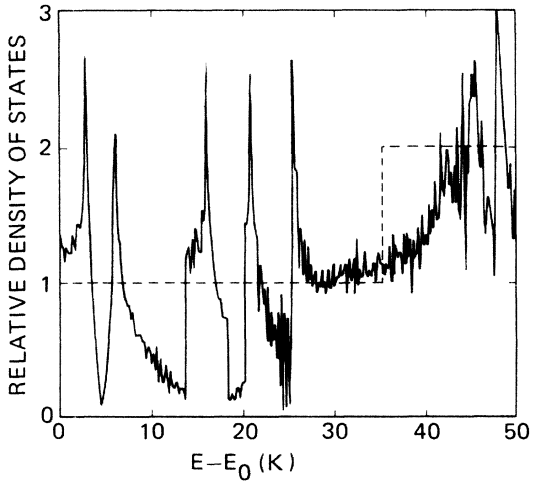

FIG. 4. Relative density of states $g(E)/g_0$, as defined in Eqs. (10) and (11) for ^{4}He on Ar-plated graphite (solid curve). Dashed line represents Eq. (11b), obtained if matrix elements of the corrugation are assumed to be zero.

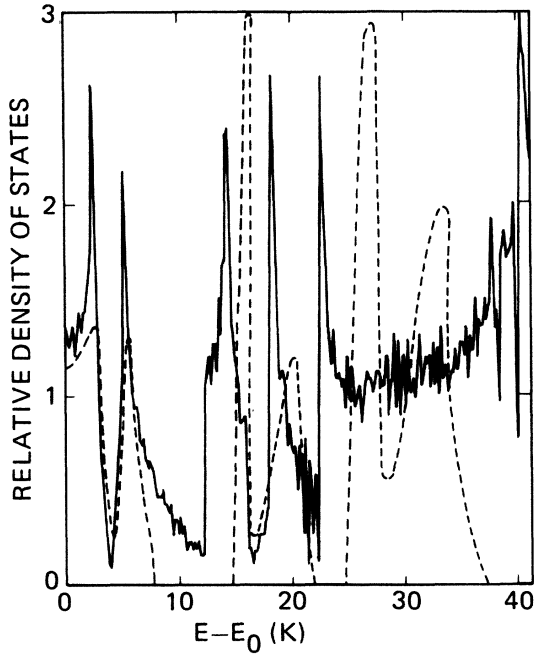

FIG. 5. Relative density of states $g(E)/g_0$ for He on Xe-plated graphite (solid curve). Dashed curve is unnormalized result of Novaco and Milford (Ref. 11) at 13% lower Xe coverage.

$$V\equiv\left\langle 0\left|\sum_{\mathbf{G}}V_{\mathbf{G}}(z)\right|0\right\rangle\ . \tag{13}$$

The distribution of levels is not the same for bare graphite, presenting a triangular array of sites, as for the overlayer, a honeycomb array. As seen in the figures, the two degenerate solutions are lower in the latter case ($V>0$) than the third solution. This degenerate pair separate, however, along the line $\overline{KM}$ so that there is no gap in $g(E)$. In contrast, for bare graphite ($V<0$) the upper state at the M point does not converge to the lower state at K, but merges instead there with a higher lying state, leaving a gap.[7]

Figure 5 compares the present results with those obtained previously by Novaco and Milford[11] (NM) for the case of a Xe overlayer. The most dramatic difference is the presence of a substantial gap ($\sim$7 K) in the work of NM. This may be attributed to their use of a 13% lower density for the Xe. The more open structure produces a more corrugated potential for the the atom. Thus the lowest band of NM is about 60% as wide as that found here.

This difference in density of states appears also in the heat capacity $C(T)$. In the limit of zero coverage, the classical expression is applicable:

$$C/Nk_B=\beta^2\frac{d^2\ln Z_1}{d\beta^2}\ , \tag{14}$$

$$Z_1=\int dE\,g(E)e^{-\beta E}\ , \tag{15}$$

$$\beta^{-1}=k_BT\ . \tag{16}$$

Figure 6 compares the present results for He on Xe-plated graphite with those of NM. We observe a substantial band-structure effect (deviation from the value

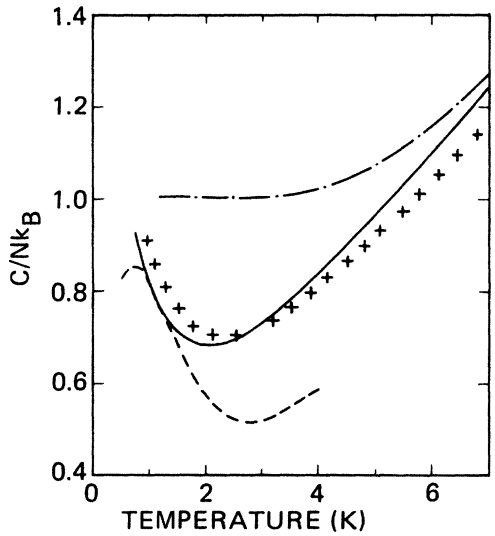

FIG. 6. Heat capacity computed from Eq. (14) for zero coverage ^{4}He on Xe-plated graphite (solid curve) compared with prediction of smooth surface model (dashed-dotted curve). Also shown is the Xe-graphite result (dashed curve) of Novaco and Milford (Ref. 11) at ^{4}He coverage 0.028 Å^{-2}. The plusses are the present prediction for the case of zero coverage He on Ar-plated graphite. The Kr case is essentially identical to that of Xe.

$C_{2D}=Nk_B$) but not so large as was obtained by NM. Note that another difference in Fig. 6 is the effect of degeneracy; i.e., at finite coverage C vanishes at $T=0$ if $N/A\neq 0$. This affects the NM results in the regime $T<2$ K. Finally, we note the expected rise at high T above the 2D value. For $T>7$ K, this is qualitatively represented by the prediction based on $g_{\rm sm}(E)$. Figure 6 shows also results for the case of Ar plating which reveal somewhat smaller band structure effects than for Xe. These are shifted to a somewhat higher T because the higher adsorbate density produces a gaplike reduction in $g(E)$ at higher energy E than occurs for Xe.

III. DISCUSSION

A set of experiments performed on plated graphite surfaces is relevant to these calculations. We refer first to the isosteric heat q_{st} measurement of Lerner and Daunt on Ar-plated graphite.[2] These authors found $q_{st}=82$ K ($\pm 5\%$) for low-coverage He data in the vicinity of $T=10$ K; from this, they estimated a binding energy in the range 57–67 K, depending on the model used. We revise this analysis as follows. At high T, the smooth surface model represents the thermal properties satisfactorily (Fig. 6). Using it allows us to calculate coexisting vapor, as appropriate for low coverage, the model yields

$$q_{st}=-\left[\frac{\partial \ln P}{\partial \beta}\right]_N, \tag{17}$$

$$q_{st}=\frac{3}{2\beta}+\frac{\sum_n |E_n| e^{-\beta E_n}}{\sum_n e^{-\beta E_n}}\equiv\frac{3}{2\beta}+f|E_0|\ . \tag{18}$$

The sums here run over the vibrational bound states. While these sums are totally dominated at very low T by the ground state (so that $f=1$), at $T=10$ K our computed values[15] yield $f=0.97$, a small correction.[22] Thus we conclude that the "experimental" value of the ground-state binding energy $|E_0|=[q_{st}-\frac{3}{2}\beta]/f$ is actually 69 K. This is about 10% higher than the value in Table I, calculated for Ar density 0.073 Å^{-2}. The difference can be interpreted in terms of the higher density in the experiment; using the value 0.087 Å^{-2} estimated by Lerner and Daunt,[2,23] we obtain[24] a ground-state energy of $|E_0|=71$ K, which is consistent with the data. The converse procedure may be used to compute q_{st} directly without resorting to the smooth surface model: in general, for zero He coverage, $q_{st}=5/(2\beta)-\bar{E}$, where $\bar{E}$ is the average energy computed from $g(E)$. This yields $q_{st}=85.8$ K at $T=10$ K, consistent with the result of Lerner and Daunt.

We turn next to the specific heat of He on Ar-plated graphite.[2–4] The data of Crary *et al.* are taken with more than a full layer of Ar. This may explain the otherwise perplexing behavior of the heat capacity in the regime $3<T<4$ K. What we refer to is that the zero-coverage extrapolation is $C/Nk_B\simeq 1.8$. This is much higher than the theoretical value ~ 0.8 in Fig. 6. Moreover, the measured[4] coverage dependence ($dC/dN<0$) is the opposite of expectation based on the virial expansion in this range of T.[5] Without presenting a quantitative analysis, we speculate that the data may indicate ^{4}He condensation in the vicinity of the Ar atoms in the second layer. Consistent with this is the fact that the ^{3}He data do not exhibit the enhanced $C(T)$, as expected from the weaker binding. We note also that the sparse data of Koutsogeorgis and Daunt[2] have $C/Nk_B\lesssim 1$ in the vicinity of 3 K, closer to the theoretical value.

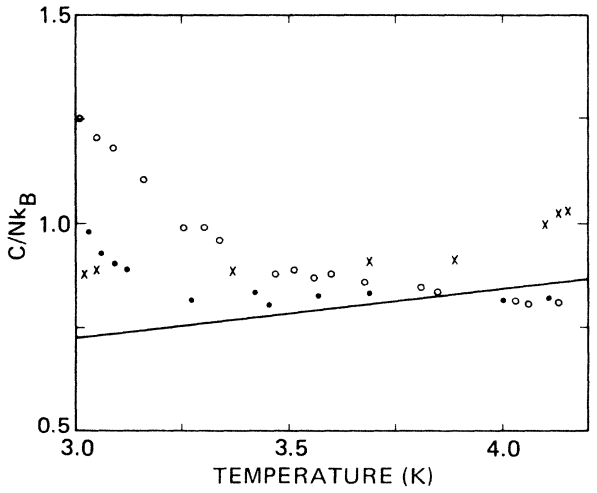

FIG. 7. Computed zero-coverage heat capacity of He on commensurate Kr on graphite (solid curve) compared with data of Tejwani (Ref. 4) at the coverages 0.0094 Å^{-2} (×), 0.015 Å^{-2} (●), and 0.023 Å^{-2} (○); these data, called Kr III in the paper of Crary *et al.* (Ref. 4) were obtained using commensurate Kr on graphite foam. Note suppressed zero on ordinate.

Finally we turn to data of Ref. 4 for ^{4}He/Kr/graphite. The results most relevant to our calculations are compared in Fig. 7 with data of Crary *et al.* At low He coverage on commensurate Kr. The lowest coverage results are seen to lie about 15% above the theoretical prediction. One may again speculate about the effect of heterogeneity as a potential explanation of the discrepancy, but we cannot test that idea quantitatively without a more substantive characterization of the heterogeneity.[9,25]

IV. SUMMARY

Calculations have been presented concerning the effects on He properties of varying the substrate. Missing from the comparison with experiment is the ability to identify accurately the state of the monolayer on which the He is adsorbed. The clearest exception, presented in Fig. 7, pertains to the commensurate Kr regime. There we find satisfactory agreement with the data of Crary *et al.* It would be of particular interest to study similarly the He $C(T)$ dependence on the Ar density. In that case we have conjectured that second layer Ar atoms are responsible for the anomalously high value of C at $T=4$ K. This is testable by employing a reduced Ar coverage. Similarly useful would be the systematic study of the isosteric heat's dependence on the density of the monolayer. The evidence presented above indicates that our calculations are consistent with the q_{st} data of Lerner and Daunt for the case of the Ar plating. It is perhaps useful to emphasize that this agreement is of some importance with respect to understanding the role of many body forces.[14–16,26] Our calculations include three-body forces in the triple dipole approximation. In the net these represent a contribution to E_0 of order $+6$ K; i.e., a substantial reduction in the He binding energy which would be predicted with only two-body forces. The relative size of this contribution is the same as that found in other bulk and surface problems.[15,16,26]

The binding energies $|E_0|$ computed by Novaco and Milford[11] are substantially larger than those appearing in Table I. Thus for Xe the NM value is $|E_0|=77$ K, more than 20% larger than our value even though the Xe density was lower. The differences are due to their omission of the repulsive triple dipole energy and their use of more attractive He-Xe and He-graphite potentials. Each of these factors contributes about the same amount to the binding-energy excess. It is seen, therefore, that adsorption data can complement surface scattering data in enhancing our understanding of noble gas interactions.

ACKNOWLEDGMENTS

We are very grateful for helpful communication to O. E. Vilches, whose experiments stimulated this work. Thanks are due also to M. Chan, J. Rehr, and A. D. Novaco for useful discussions and to S. Crary for noticing a mistake in a figure. This work was supported in part by the National Science Foundation under Grant No. DMR-84-19261.

[1]O. E. Vilches, Ann. Rev. Phys. Chem. **31**, 463 (1980); S. B. Crary and O. E. Vilches, Phys. Rev. Lett. **38**, 973 (1977); M. J. Tejwani, O. Ferreira, and O. E. Vilches, *ibid.* **44**, 152 (1980).

[2]E. Lerner and J. G. Daunt, J. Low Temp. Phys. **10**, 299 (1973); **41**, 629 (1980); C. N. Koutsogeorgis and J. G. Daunt, J. Phys. (Paris) Colloq. **39**, C6-308 (1978).

[3]M. Bretz, J. G. Dash, D. C. Hickernell, E. O. McLean, and O. E. Vilches, Phys. Rev. A **8**, 1589 (1973); S. E. Polanco and M. Bretz, Phys. Rev. B **17**, 151 (1978).

[4]S. B. Crary, O. Ferreira, M. J. Tejwani, and O. E. Vilches (unpublished); S. B. Crary, thesis, University of Washington, 1978; M. J. Tejwani, thesis, University of Washington, 1979; O. Ferreira, thesis, University of Campinas, Brazil, 1978.

[5]J. J. Rehr and M. J. Tejwani, Phys. Rev. B **19**, 345 (1979); E. V. L. deMello and J. J. Rehr (unpublished).

[6]J. G. Dash and M. Schick, in *The Physics of Liquid and Solid Helium, Part II,* edited by K. H. Bennemann and J. B. Keterson (Wiley, New York, 1978), p. 497.

[7]W. E. Carlos and M. W. Cole, Phys. Rev. B **21**, 3713 (1980).

[8]L. W. Bruch, Phys. Rev. B **23**, 6801 (1981); Z.-C. Guo and L. W. Bruch, J. Chem. Phys. **77**, 1417 (1982); G. Vidali and M. W. Cole, Phys. Rev. B **22**, 4661 (1980); **23**, 5649 (1981).

[9]R. L. Elgin and D. L. Goodstein, Phys. Rev. A **9**, 2657 (1974); A. F. Silva-Moreira, J. L. Codona, and D. L. Goodstein, Phys. Lett. **76A**, 324 (1980); M. W. Cole, D. R. Frankl, and D. L. Goodstein, Rev. Mod. Phys. **53**, 199 (1981).

[10]F. J. Milford and A. D. Novaco, Phys. Rev. **14**, 1136 (1971).

[11]A. D. Novaco and F. J. Milford, Phys. Rev. A **5**, 783 (1972); **6**, 526(E) (1972).

[12]R. Aziz, in *Inert Gases,* Vol. 34 of *Springer Series in Chemical Physics,* edited by M. L. Klein (Springer, New York, 1984).

[13]G. Vidali, M. W. Cole, and C. Schwartz, Surf. Sci. **87**, L273 (1979).

[14]J. M. Hutson and C. Schwartz, J. Chem. Phys. **79**, 5179 (1983).

[15]S. Chung, N. Holter, and M. W. Cole, Phys. Rev. B **31**, 6660 (1985); Surf. Sci. **165**, 466 (1986).

[16]C. Schwartz (unpublished).

[17]J. Z. Larese, W. Y. Leung, D. R. Frankl, S. Chung, and M. W. Cole, Phys. Rev. Lett. **54**, 2533 (1985); G. Bracco, P. Cantini, E. Cavanna, R. Tatarek, and A. Glachant, Surf. Sci. **136**, 169 (1984).

[18]H. Taub, K. Carneiro, J. K. Kjems, L. Passell, and J. P. McTague, Phys. Rev. B **16**, 4551 (1977), report density of this order for Ar.

[19]G. Derry, D. Wesner, W. E. Carlos, and D. R. Frankl, Surf. Sci. **87**, 629 (1979); S. Chung, A. Kara, and D. R. Frankl (unpublished); G. P. Boato, P. Cantini, C. Guidi, R. Tatarek, and G. P. Felcher, Phys. Rev. B **20**, 3957 (1979).

[20]J. W. Cooley, Math. Comput. **15**, 363 (1961); J. K. Cashion, J. Chem. Phys. **33**, 1872 (1963); R. J. Le Roy, University of

Waterloo Chemistry and Physics Research Reprint No. CP-230R, 1983 (unpublished).

[21]C. C. Maitland and E. B. Smith, Chem. Phys. Lett. **22**, 443 (1983); K. M. Smith, A. M. Rulis, G. Scoles, R. A. Aziz, and V. Nain, J. Chem. Phys. **67**, 152 (1977).

[22]This correction is only weakly dependent on model; its low T form is $f \rightarrow 1+(\delta/\varepsilon_0)\exp(-\beta\delta)$, where $\delta=\varepsilon_1-\varepsilon_0\sim 30$ K in the present case.

[23]E. Lerner and J. G. Daunt, J. Low. Temp. Phys. **6**, 241 (1972).

[24]This energy shift may be estimated from the $|dE_0/d\theta| \simeq 3.7$ meV in Ref. 15 and $\Delta\theta=0.22$ (commensurate layers) difference in density.

[25]R. E. Ecke, J. G. Dash, and R. D. Puff, Phys. Rev. B **26**, 1288 (1982).

[26]W. J. Meath and R. A. Aziz, Mol. Phys. **52**, 225 (1984).